# THE 180 DEGREE REFLECTIVITY AND VELOCITY PERTURBATION OF THIN METAL DOTS

F. HUANG, E. G. S. PAIGE AND D. R. SELVIAH

Department of Engineering Science
University of Oxford
England

## Abstract

Reflective arrays of rectangular thin metal 'dots' spaced in a regular or near regular grid pattern, such as have been used in surface acoustic wave resonators [1] and in-line dot RACs [2] on $LiNbO_3$, are analysed. The half wavelength spacing of dots required leads to capacitative coupling between adjacent dots. The charge distribution induced on the dots by the passage of the SAW is presented including the coupling. The 180° SAW reflectivity of the dots and the SAW velocity perturbation through the dot array are given for a range of dot sizes. These are shown to be in good agreement with experimental results [1].

The work establishes that the method of analysis can form the basis of the design of 180° reflective weighted dot arrays allowing them to be implemented through varying dot density and/or by varying dot dimensions.

## 1. Introduction

Electronic devices based on the reflection of surface acoustic waves (SAWs) by reflective array structures are of importance in signal processing applications. This paper concentrates on those devices in which the SAWs are reflected through 180°. Such devices include SAW resonators [1] and In-Line Reflective Array Compressors (ILRACs) [2].

A variety of SAW reflectors have been used within the reflecting arrays including grooves, [3], thin metal strips [4], thick metal dots [5] and more recently thin metal dots [6]. The thin metal dots have a number of practical advantages over other techniques:

(i) They are very simple to fabricate unlike grooves; only a single lithographic step being required to fabricate both transducers and reflective thin metal dot arrays.

(ii) Very tight tolerances on metal thickness are not required since the reflection mechanism is based on the electrical shorting effect unlike thick metal dots where the reflectivity depends predominantly on the mass loading and hence thickness. Thin metal dots simply need to be thin enough to avoid mass loading (thickness $< 0.005\ \lambda$) and yet thick enough to provide a conducting region.

(iii) Thin metal dots arrays can give lower loss. In metal strip arrays modes are set up in which charge flows along the length of the strip leading to ohmic loss. In metal dot arrays this is avoided resulting in higher Q's in resonators [1]. Dot arrays have about 1/5th of the loss of strip arrays. In addition multistrip coupler type behaviour can be avoided.

Although impressive results have been obtained for both resonators and ILRACs employing SAW 180° reflective thin metal dot arrays, a theoretical basis that enables weighted arrays to be accurately designed has not been available. For even if the dot density in a reflecting row is used as the basis for designing in reflectivity weighting [5], effects of mutual coupling and of velocity perturbation are overlooked. It is the aim of the paper to present a theoretical model and resulting design curves for 180° reflectivity and velocity perturbation to enable such weighted arrays to be designed. In section 2, a model is described for the reflection of SAWs from thin metal dot arrays taking full account of the electrical interactions between dots. Section 3 compares the theoretical predictions of the model with experimental results obtained from SAW resonators on lithium niobate. Good agreement is obtained. Section 4 presents sets of design curves for both sparse and more dense arrays. The paper concludes with a discussion and summary in section 5.

## 2. Theoretical Model including Interactions

The model is an adaptation of that successfully employed for 90° reflections from thin metal dots arrays [6]. Two cases of interest are considered in this section:

(i) SAWs incident normally on one free face of an isolated rectangular metal dot

(ii) SAWs incident on a dot array (see Figure 1) where the dots are assumed to lie on reflecting rows normal to the propagation direction and columns parallel to the propagation direction and the dot faces are aligned with the rows and columns. The row separation is chosen to be $\lambda_o/2$ so that 180° reflections add in phase as in typical resonator and ILRAC structures. The

0090-5607/85/0000-0011 $1.00 © 1985 IEEE

column spacing is also chosen to be $\lambda_0/2$ making what has been termed, a 'waffle iron' array [1].

The model and calculation can conveniently be divided into two parts:

(i) Calculation of the charge distribution on the dot.

(ii) Calculation of the scattered SAW field.

### 2.1 Charge distribution calculation

On a piezoelectric substrate a SAW is accompanied by a potential wave with the same velocity and wavelength. As the SAW with its associated potential passes through a metallic dot the charge on the dot flows so as to maintain a constant potential over the dot. The charge distribution on the dot is found by treating the problem as purely electrostatic. That is:-

(i) Assume the dot has a potential $V_m$ at some instant.

(ii) Find the difference between the potential $V_m$ on a surface with a dot present and that which would have prevailed on a free surface at the same instant

$$\Delta V = V_m - V_0 \cos(\omega t - kx) \qquad (1)$$

where $\omega$ and k are the angular frequency and wave vector respectively and $V_0$ is the peak potential of the wave.

(iii) Attribute the potential difference to redistribution of charge on the dot. This difference potential must therefore be generated by the repositioned charge on the dot.

(iv) Subdivide the dot into rectangular cells, the jth cell containing a charge $q_j$. Then the difference potential $\Delta V_i$ on the ith cell is due to the charge in all the cells of the dot itself and the charge in all the cells of neighbouring dots, so taking account of electrostatic coupling between dots. This can be expressed in matrix formalism:

$$\Delta V_i = M_{ij} q_j \qquad (2)$$

where $M_{ij}$ comes directly from the potential given by a charge.

(v) Solve this equation for $q_j$ by matrix inversion and find $V_m$ with the aid of charge conservation (total charge on the dot is zero) to yield the charge distribution on the dot $q_j$ and the dot potential $V_m$.

Since the dot is a thin lamina and it is known that charge tends to concentrate near edges and points, it may be expected that charge would build up along the dot edges and particularly at the corners. Thus the calculated charge distribution in Figures 2 and 3 for an isolated dot, one face being normal to the incident SAW beam, is much as expected. The dot has a length parallel to the incident SAW of $a = 0.5\lambda_0$ and a width normal to the incident SAW of $b = 0.25\lambda_0$ where $\lambda_0$ is the incident SAW wavelength. Figures 2 and 3 show the charge distribution at two instants when the SAW potential wave lies symmetrically under the dot and antisymmetrically. For similar dots within a 'waffle iron' array the charge is enhanced at the dot ends in the symmetric case and suppressed in the antisymmetric case due to coupling.

### 2.2 Scattered SAW field calculation

By extending the one dimensional analysis of Milsom et al [7] and Morgan [8] to two dimensions an oscillatory point charge generates a scattered SAW field given by the point SAW Green's function, G. When the radiating source is, however, a charge distribution the scattered SAW potential is given by

$$\bar{V}(\underline{k}) = \bar{G}(\underline{k}).\bar{\sigma}(\underline{k}) \qquad (3)$$

where these quantities are the two dimensional Fourier transforms of the equivalent quantities as a function of distance. Therefore, at any point in the SAW radiation field, the SAW amplitude and phase are found by summing the contributions from the point SAW Green's functions due to the point charges within each rectangular cell of the dot taking account of relevant phase delays.

The forward scattered wave is 90° out of phase relative to the incident wave. This gives an overall phase shift after the wave has traversed one row of dots. A similar phase shift occurs at each row resulting in an effective velocity reduction in a waffle iron array. The fractional velocity perturbation is given in terms of the forward scattered reflectivity r(0°) by

$$\frac{\Delta V}{V} = 2r(0°)/\pi \qquad (4)$$

## 3. Comparison of Model Predictions with Experimental Waffle Iron Results

Matthaei and Barman [1] have performed several experiments on waffle iron configurations in which they placed rectangular dots on a regular square lattice of periodicity $\lambda_0/2$ (Figure 1) and investigated the velocity perturbation and 180° reflectivity as they varied the dot length, a, parallel to the propagation direction whilst maintaining the dot width normal to the propagation direction at $b = \lambda_0/4$. They only considered frequencies resonant with the structure i.e. SAWs of wavelength $\lambda = \lambda_0$.

The waffle iron structure has been treated using the model described in Section 2. In order to take full account of the electrostatic coupling between dots the number of near neighbour interactions was increased until the inclusion of further interactions produced negligible change. In the worst case (nearly touching dots) this required 20 near neighbours to be included.

Following Matthaei and Barman the 'Fractional

column metallisation', t, is defined to be

$$t = a/(a+g) \qquad (5)$$

Figure 4 shows how model predictions of the variation of 180° reflectivity of a waffle iron dot row as the dot length, a, is increased is in good agreement with the experiment. Figure 5 also shows similar good agreement between experiment and theory for the fractional velocity change.

## 4. Design Curves

Figures 6 and 7 have been calculated for a waffle iron array as described above. The curves show contours of constant 180° reflectivity and 0° forward scattering as a function of dot length (a) and dot width (b). For the range of dot dimensions plotted, interactions between dots were found to be weak. The strongest interactions were found between adjacent dots in the same column so that, compared to an isolated dot, the greatest difference in reflectivity occurred at $a = 0.4\lambda$, $b = 0.4\lambda$. For this case the waffle iron had a reflectivity of 2.55% compared with 2.25% for the isolated dot and velocity perturbation of -1.43% compared with -1.62%. Thus these curves can be used as universal design curves for dot arrays with a $\lambda_0/2$ spacing parallel to the propagation direction and a spacing greater than or equal to $\lambda_0/2$ along the rows themselves since for the ranges specified the interaction between adjacent dots in the same row are negligible. (For normallization purposes, the separation between dots in a row has been taken as $1\lambda_0$.) Figures 8 and 9 show similar curves for isolated dots over a much wider range of dimensions. These curves can therefore be used to design sparse dot arrays where interactions are small.

## 5. Discussion and Conclusions

The velocity perturbation and 180° reflectivity of thin rectangular metal dots both when isolated and in a waffle iron array have been predicted, and predictions have been found to be in very good agreement with the experimental results available. This provides validation of the theoretical method. Predictions have then been extended to form a basis for designing arrays with chosen properties e.g. reflectivity as a function of dot dimensions for the purposes of weighting. The universal design curves presented are valid for a row spacing of $\lambda_0/2$ which is suitable for resonators and ILRACs.

During fabrication slight changes in the dot dimensions can occur as a result of over or under etching. When this occurs both a and b can be expected to decrease or increase by the same amount. By choosing the dot dimensions to lie on one of the contours at the point where the contour becomes a tangent to the line a = b the dot reflectivity will be most insensitive to fabrication tolerances. This feature, which can lead to an improvement in reproducibility, is not available for simple strip arrays.

This new form of weighting can be combined with other weighting techniques such as dot density [9], phase weighting, withdrawal weighting and row length weighting [10].

New forms of array structure can also be accommodated such as those using reflectors having alternate polarity reflection coefficients recently described [11]. To date grooves and ridges or shorted and open metal strips have been considered. Figure 8 shows that by choosing dot dimensions suitably, dots with both positive and negative reflection coefficients can be realised.

## 6. References


1. Matthaei, G. L. and Barman, F., 'A study of the Q and Modes of SAW resonators using metal "waffle-iron" and strip arrays', IEEE Transactions on Sonics and Ultrasonics, Vol. SU-25, No. 3, pp. 138-146, May 1978.

2. Woods, R. C., 'Reflective array compressors using 180° reflecting metal dot arrays', J. Appl. Phys., Vol. 54, No. 11, November 1983.

3. Chapman, R. E., Chapman, R. K., Morgan, D. P. and Paige, E. G. S., 'In-Line Reflective Array Devices', 1978 IEEE Ultrasonics Symposium, pp 728-733.

4. Riha, G., Stocker, H. R., Veith, R. and Bulst, W. E., 'RAC-filters with position weighted metallic strip arrays', 1982 IEEE Ultrasonics Symposium, pp 83-87.

5. Solie, L. P., 'Surface acoustic wave reflective dot array (RDA), Applied Physics Letters, Vol. 28, No. 8, pp 420-422, 1976

6. Huang, F. and Paige, E. G. S., 'Reflection of surface acoustic waves by thin metal dots', 1982 IEEE Ultrasonics Symposium Proceedings, pp 72-82.

7. Milsom, R. F, Reilly, N. H. C. and Redwood, M. 'Analysis of generation and detection of surface and bulk acoustic waves by interdigital transducers', IEEE Transactions on Sonics and Ultrasonics, Vol SU-24, No 3, pp 147-166, May 1977.

8. Morgan, D. P., 'Quasistatic analysis of generalised SAW transducers using the Green's Function method', IEEE Transactions on Sonics and Ultrasonics, Vol SU-27, pp 111-123, No 3, May 1980.

9. Tanski, W. J.; Block, M. and Vulcan, A., 'High performance SAW resonator filters for satellite use', 1980 IEEE Ultrasonics Symposium Proceedings, pp 140-152.

10. Edmonson, P. J.; Campbell, C. K. and Smith, P. M., 'Narrow-band SAW filters using stepped-resonators with tapered gratings', 1984 IEEE Ultrasonics Symposium, pp 235-238.

11. Yamanouchi, K. and Furuyashiki, H., 'Low-loss SAW filter using internal reflection types of new single-phase unidirectional transducer', 1984 IEEE Ultrasonics Symposium, pp 68-71.

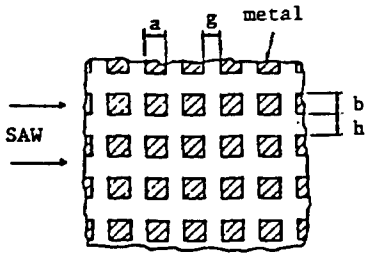


Figure 1. Waffle iron reflective array.

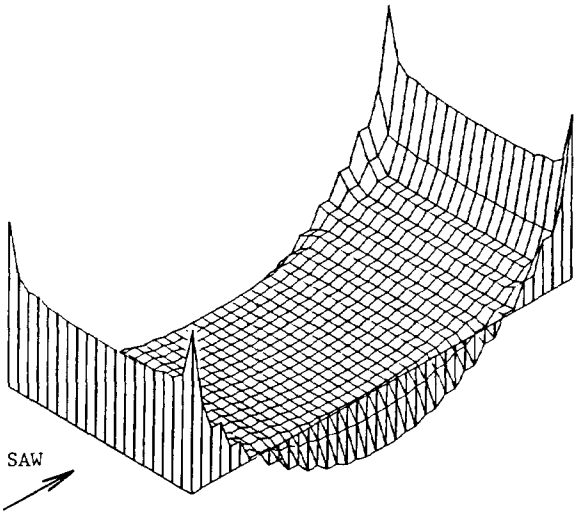


Figure 2. Charge distribution on a dot with $a = 0.5\lambda_0$ and $b = 0.25\lambda_0$ - SAW potential symmetrical with respect to dot.

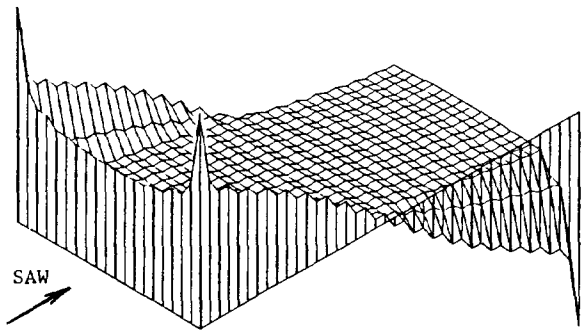


Figure 3. Charge distribution on a dot with $a = 0.5\lambda_0$ and $b = 0.25\lambda_0$ - SAW potential antisymmetrical with respect to dot.

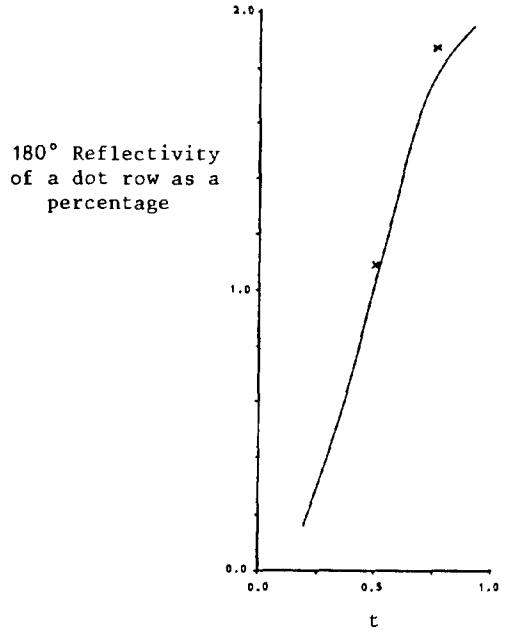


Figure 4. 180° reflectivity as a function of metallization for waffle iron array; theory (——), experiment (x x).

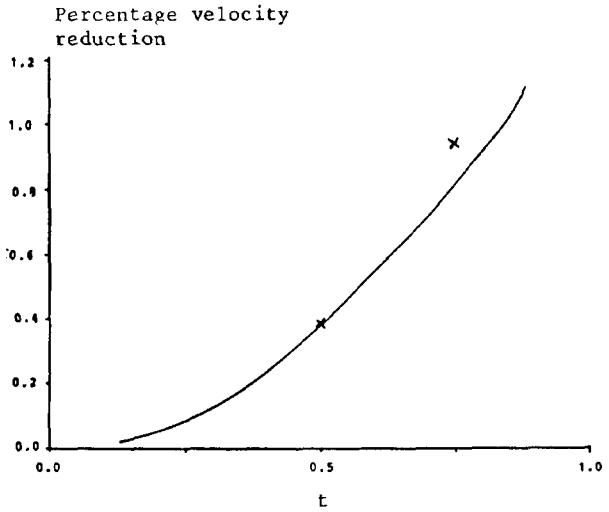


Figure 5. Velocity change as a funciton of metallization for a waffle iron array; theory (——), experiment (x x)

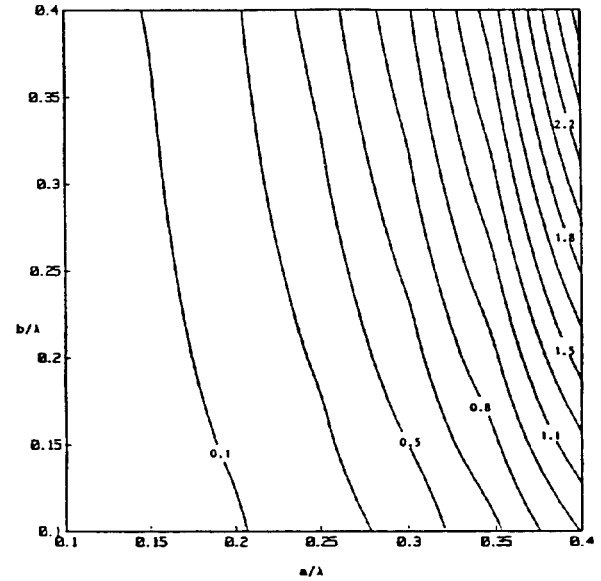


Figure 6. 180° reflectivity (percentage) as a function of dot dimensions for a waffle iron array with row period of of $\lambda_0/2$.

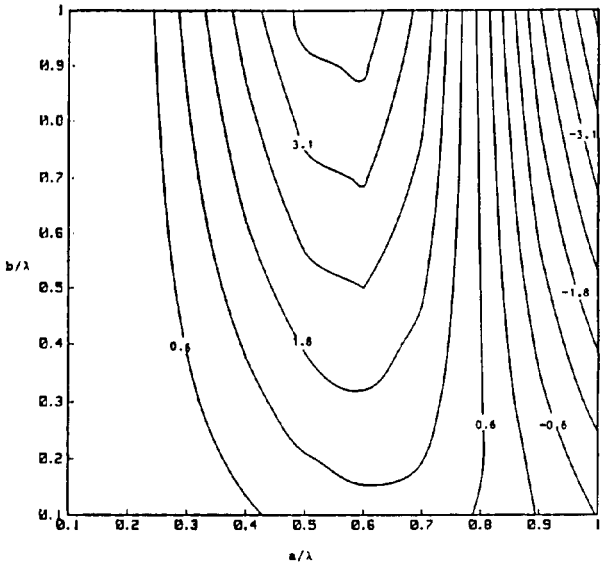


Figure 8. 180° reflectivity (percentage) as a function of dot dimension for a single row of dots.

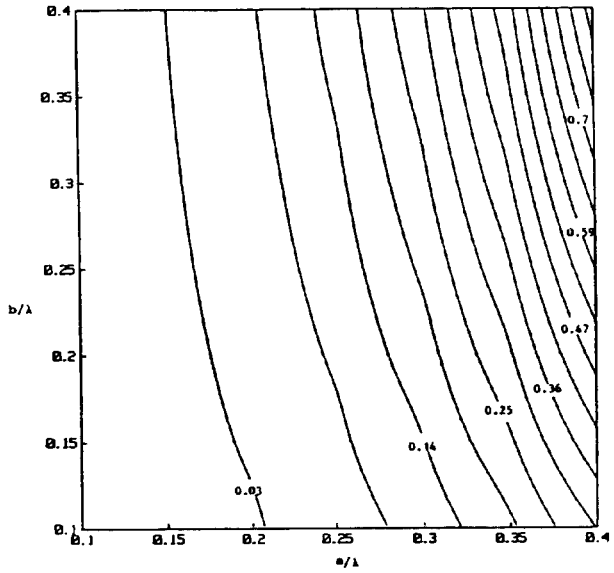


Figure 7. Percentage velocity reduction as a function of dot dimensions for a waffle iron array with row period of $\lambda_0/2$.

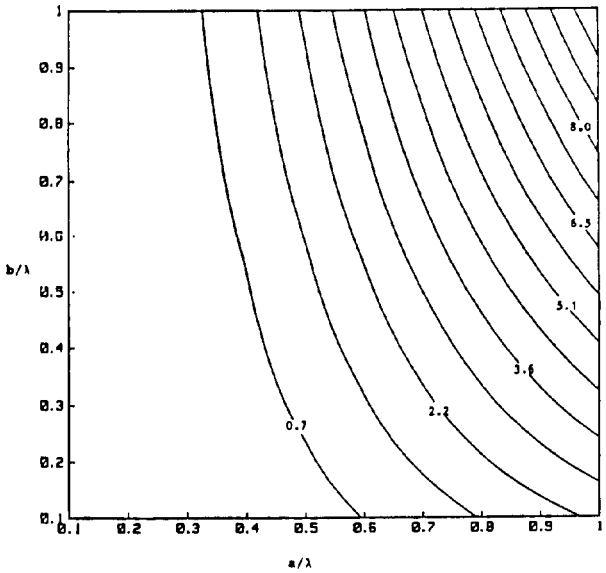


Figure 9. Percentage velocity reduction as a function of dot dimensions for a single row of dots.